and this must be normal to $\tau(\Pi)$ in S. Hence

$$(p_{r-1}\mathbf{e}_0 - p_r\mathbf{e}_1 + p_1\mathbf{e}_r).\ (\mathbf{e}_1 \sin 2\pi/n + \mathbf{e}_r \sin 2\pi r/n) = 0$$

giving

$$p_1/(\sin 2\pi/n) = p_r/(\sin 2\pi r/n).$$

Since the area of a rhombus of the rth kind with unit sides is $\sin 2\pi r/n$, it follows that the frequency with which the different kinds of rhombi occur is in proportion to their areas. For all values of $n \neq 3$, 4 or 6 some ratios of $\sin 2\pi/n : \sin 2\pi r/n$ are irrational, which conforms with an earlier proof of the non-periodicity of Penrose tilings.

References

BENDERSKY, L. (1985). *Phys. Rev. Lett.* **55**, 1461-1467.

BRUIJN, N. G. DE (1981). *Proc. K. Ned. Akad. Wet. Ser. A*, **43**, 39-66.

DUNEAU, M. & KATZ, A. (1985). *Phys. Rev. Lett.* **54**, 2688-2691.

FUNG, K. K., YANG, C. Y., ZHOU, Y. Q., ZHAO, J. G., ZHAN, W. S. & SHEN, B. G. (1986). *Phys. Rev. Lett.* **56**, 2060-2063.

GÄHLER, F. & RHYNER, J. (1986). *J. Phys. A*, **19**, 267-277.

GRÜNBAUM, B. & SHEPHERD, G. C. (1987). *Tilings and Patterns.* New York: W. H. Freeman.

ISHIMASA, T., NISSEN, H. U. & FUKANO, Y. (1985). *Phys. Rev. Lett.* **55**, 511-513.

KRAMER, P. & NERI, R. (1984). *Acta Cryst.* A**40**, 580-587.

MACKAY, A. L. (1982). *Physica (Utrecht)*, **114A**, 609-613.

PAULING, L. (1987). *Phys. Rev. Lett.* **58**, 365-368.

PENROSE, R. (1978). *Eureka*, **39**, 16-22.

SCHECHTMAN, I., BLECH, D., GRATIAS, D. & CAHN, H. W. (1984). *Phys. Rev. Lett.* **53**, 1951-1954.

VENKATARAMAN, G. (1985). *Bull. Mater. Sci.* **7**, 179-199.

WATANABE, Y., ITO, M. & SOAMA, T. (1987). *Acta Cryst.* A**43**, 133-134.

WHITTAKER, E. J. W. & WHITTAKER, R. M. (1986). *Acta Cryst.* A**42**, 387-398.

Acta Cryst. (1988). A**44**, 112-123

Restrained Refinement of Two Crystalline Forms of Yeast Aspartic Acid and Phenylalanine Transfer RNA Crystals

BY E. WESTHOF, PH. DUMAS AND D. MORAS

Laboratoire de Cristallographie Biologique, Institut de Biologie Moléculaire et Cellulaire, Centre National de la Recherche Scientifique, 67084 *Strasbourg CEDEX, France*

(*Received* 21 *January* 1987; *accepted* 8 *May* 1987)

Abstract

Four transfer RNA crystals, the monoclinic and orthorhombic forms of yeast $tRNA^{Phe}$ as well as forms *A* and *B* of yeast $tRNA^{Asp}$, have been submitted to the same restrained least-squares refinement program and refined to an *R* factor well below 20% for about 4500 reflections between 10 and 3 Å. In yeast $tRNA^{Asp}$ crystals the molecules exist as dimers with base pairings of the anticodon (AC) triplets and labilization of the tertiary interaction between one invariant guanine of the dihydrouridine (D) loop and the invariant cytosine of the thymine (T) loop (G19-C56). In yeast $tRNA^{Phe}$ crystals, the molecules exist as monomers with only weak intermolecular packing contacts between symmetry-related molecules. Despite this, the tertiary folds of the *L*-shaped tRNA structures are identical when allowance is made for base sequence changes between $tRNA^{Phe}$ and $tRNA^{Asp}$. However, the relative mobilities of two regions are inverse in the two structures with the AC loop more mobile than the D loop in $tRNA^{Phe}$ and the D loop more mobile than the AC loop in $tRNA^{Asp}$. In addition, the T loop becomes mobile in $tRNA^{Asp}$. The present refinements were performed to exclude packing effects or refinement bias as possible sources of such differential dynamic behavior. It is concluded that the transfer of flexibility from the anticodon to the D- and T-loop region in $tRNA^{Asp}$ is not a crystalline artefact. Further, analysis of the four structures supports a mechanism for the flexibility transfer through base stacking in the AC loop and concomitant variations in twist angles between base pairs of the anticodon helix which propagate up to the D- and T-loop region.

1. Introduction

Biological macromolecules often present crystalline polymorphism and this effect is particularly pronounced with tRNA molecules (Dock, Lorber, Moras, Pixa, Thierry & Giegé, 1984). Such a polymorphism offers the possibility of studying different conformational states of the molecules. The crystal structures of two crystal forms of yeast aspartic acid tRNA ($tRNA^{Asp}$) have recently been refined to an *R* factor below 20% at 3 Å resolution (Westhof, Dumas & Moras, 1985; Dumas, Westhof & Moras, 1988). For these refinements, a restrained least-squares program,

0108-7673/88/020112-12$03.00

originally developed for the refinement of protein structures (Konnert, 1976; Hendrickson & Konnert, 1980; Konnert & Hendrickson, 1980), was modified to apply to nucleic acids in the form *NUCLIN* and *NUCLSQ* (Westhof, Dumas & Moras, 1985). Although belonging to the same space group, the two forms of yeast $tRNA^{Asp}$ are non-isomorphous and significant differences could be identified in the D loop (Dumas, Westhof & Moras, 1988). In form *B*, the D loop interacts with the T loop through intercalation of one guanine; while, in form *A*, there is in addition hydrogen bonding between the next guanine and C56 of the T loop. On the other hand, yeast phenylalanine tRNA ($tRNA^{Phe}$) which has been refined in the monoclinic form (Hingerty, Brown & Jack, 1978) and in the orthorhombic form (Sussman, Holbrook, Wade Warrant, Church & Kim, 1978; Quigley, Teeter & Rich, 1978) does not differ significantly in the two forms. For the latter form, the program *CORELS* (Sussman, Holbrook, Church & Kim, 1977) was used and, for the former one, a program combining energy and least-squares refinement (Jack & Levitt, 1978) was employed, as well as least-squares restrained refinement (Quigley, Teeter & Rich, 1978; Konnert & Hendrickson, 1980).

Because tRNA molecules can interact with other macromolecules either extremely specifically (for example with their cognate aminoacyltRNA synthetase) or without specificity (for example in their interactions with ribosomal A and P sites), careful comparison studies are necessary for disentangling the underlying structural features responsible for the specificity of each tRNA from those features maintaining the overall three-dimensional *L*-shaped folding of elongated tRNA molecules. Besides, the crystal structure of yeast $tRNA^{Asp}$ (Moras, Comarmond, Fischer, Weiss, Thierry, Ebel & Giegé, 1980) led to the suggestion that the molecular structure of yeast $tRNA^{Asp}$ is a model for a tRNA molecule bound to a messenger codon triplet while that of yeast $tRNA^{Phe}$ is a model for the unbound tRNA molecule (Moras, Dock, Dumas, Westhof, Romby, Ebel & Giegé, 1986). Indeed, in the crystals, the yeast $tRNA^{Asp}$ molecules exist as dimers associated through base pairing of their almost self-complementary –GUC– anticodon triplets.

Some comparisons have already been made between the structure of yeast $tRNA^{Asp}$ and that of yeast $tRNA^{Phe}$ (Westhof, Dumas & Moras, 1983, 1985; Dumas, Ebel, Giegé, Moras, Thierry & Westhof, 1985; Moras *et al.*, 1986; Dumas *et al.*, 1988). However, some artefactual differences between the compared structures might arise from the crystallographic refinement method used since, as the resolution is not atomic, the lack of data has to be completed by additional observational restraints (Waser, 1963; Konnert, 1976). In order to minimize those differences, the orthorhombic form of yeast $tRNA^{Phe}$ (Sussman *et al.*, 1978) has been re-refined with *NUCLIN* and *NUCLSQ* and a monoclinic form of yeast $tRNA^{Phe}$ was further refined (Stout, Mizuno, Rao, Swaminathan, Rubin, Brennan & Sundaralingam, 1978; Westhof & Sundaralingam, 1986). Here we shall describe the refinement behavior with inclusion of solvent molecules of two forms of yeast $tRNA^{Asp}$ and the re-refinement of two forms of yeast $tRNA^{Phe}$ with the redetermination of solvent molecules. Some structural features of the four tRNA structures will be compared. A comparative discussion on the number and positions of the solvent molecules will be published elsewhere (Westhof, Dumas & Moras, 1988).

2. Restrained least squares

The refinement method has been described by Hendrickson & Konnert (1980). The programs *NUCLIN* and *NUCLSQ* have been discussed (Westhof, Dumas & Moras, 1985). In order to improve the ratio of observations to parameters, restraints were applied to covalent bond lengths and bond angles, chirality of sugar atoms, non-bonded repulsive contacts, hydrogen-bond distances and sugar puckers. The use of 'soft' and 'strong' chiral-volume restraints for maintaining proper geometry and stereochemistry in the sugar rings was described previously (Westhof & Sundaralingam, 1983; Westhof, Dumas & Moras, 1985). 'Soft' restraints (*i.e.* the chemically meaningful chiral volumes around the ring) are quite insensitive to sugar pucker, while the 'strong' restraints (*i.e. ad hoc* intra-ring chiral volumes for each of the five atoms of the sugar ring) depend strongly on sugar pucker (Fig. 1). The use of 'strong' restraints (with adequate weights) ensures correct sugar puckers, once the sugar-pucker type has been chosen. This is the case in refinements of transfer RNA molecules at 3 Å resolution, since subtle variations in each pucker domain (C2′-*endo* or C3′-*endo*) cannot be detected. The type of pucker itself is, in most cases, apparent from inspection of the electron density maps because of the different shapes of those two puckers, because of the different extensions of the two types of nucleotides, and because of the relative orientation of the base with respect to the sugar itself (Sundaralingam, 1969).

The initial overall temperature factor (which is on a relative scale) is difficult to set with data dominated by the disordered solvent at low resolution and weak at high resolution. The initial overall temperature factor was chosen so that $\sum F_{obs}/\sum F_{calc}$ was close to one, with the scale factor between F_{obs} and F_{calc} given by $\sum F_{obs}F_{calc}/\sum F_{calc}F_{calc}$, and after the application of overall temperature factor and scale shifts in successive cycles. Except at the beginning of each refinement, the temperature factors were not restrained (see below). When the *R* factor reached

20-23%, three cycles of refinement were made with the occupancy of all the atoms of the molecule variable (with temperature factors fixed). An average occupancy for each group of those residues was then used in the continuation of the refinement (see below). Afterwards, the solvent molecules were picked in ($F_{obs} - F_{calc}$) maps. Cycles of refinement were then made alternately with temperature-factor variation and occupancy variation for the solvent with starting values of about 30 Å^2 and 1·0, respectively. For form *A* of yeast tRNA^{Asp}, the occupancy was first refined and if, after three cycles, the occupancy of a solvent peak was still equal to 1·0, its temperature factor was decreased by 5 Å^2. Since these two factors are in a least-squares sense highly correlated, the effect on the overall *R* factor of refining alternately both the temperature factor and the occupancy of the solvent peak is minimal. However, these two factors might reflect different physical phenomena and their determination might be important for future comparisons with theoretical calculations and for our understanding of the solvation shell around macromolecules. The refinement was halted when no stereochemically and chemically meaningful peaks appeared in the peak lists of the difference maps. The fact that several solvent peaks were found at similar positions in all four structures argues for the validity of the method, despite the certainty that some individual peaks in each structure are noise (Westhof, Dumas & Moras, 1988). At the end of the refinement, three cycles of refinement were made with the occupancy of all atoms variable and three final cycles of refinement were made with the group average of the occupancies obtained for those residues with occupancies less than 90%.

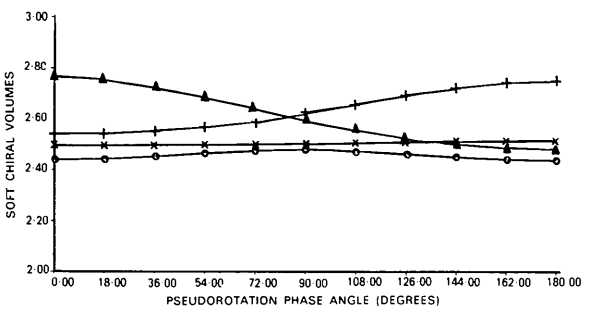

(*a*)

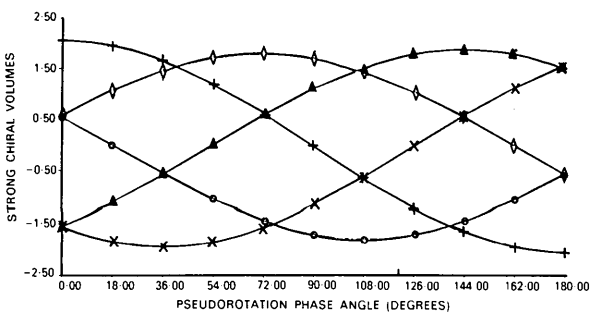

(*b*)

Fig. 1. (*a*) Variation with the phase angle of pseudorotation (*P*), as defined by Altona & Sundaralingam (1972), of the 'soft' chiral volumes at carbon atoms C(1'), ○, C(2'), ▲, C(3'), +, and C(4'), ×. (*b*) Variation with the phase angle of pseudorotation of the 'strong' chiral volumes at atoms C(1'), ○, C(2'), ▲, C(3'), +, C(4'), ×, and O(4'), ◇. These values were computed with the coordinates of the sugar ring as given by Merritt & Sundaralingam (1985).

3. Refinement parameters

The shell of diffraction data used in the refinement is that between 10 and 3 Å for each tRNA structure at the 3σ level for the tRNA^{Phe} structures and at the 2σ level for the tRNA^{Asp} structures. This gave about the same number of reflections for each structure (see Table 1). A plot of the variation of the mean value of observed structure factors as a function of $(\sin\theta)/\lambda$ is shown in Fig. 2. The behavior of each data set as a function of resolution is slightly different: the mean F_{obs} of the orthorhombic form of tRNA^{Phe} slowly decreases with resolution up to 3·3 Å resolution and then drops abruptly; for the monoclinic form, the data fall sharply with resolution; and for the tRNA^{Asp} after some strong variations at low resolution the data vary in a way similar to the orthorhombic form of tRNA^{Phe}. The weights applied in the refinement were chosen according to the current value of the (F_{obs}-F_{calc}) difference at high resolution and were independent of the resolution. Despite the different magnitudes of the structure factors of the three crystals, the weights applied were proportionately the same. A summary of the refinement parameters for all three structures is given in Table 1. It can be seen that the refinement converged to similar *R* factors slightly below 20%, with a similar number of solvent molecules and average temperature factor. The correlation coefficients between F_{obs} and F_{calc} for the four structures are around 90%.

The agreement statistics for the geometrical and stereochemical parameters of the three structures are given in Table 2. The r.m.s. values for each given parameter are all very similar. The r.m.s. values for the difference in isotropic thermal factors for bonded and next-neighbor atom pairs are interesting to analyze. The lowest values are those of the orthorhombic form of tRNA^{Phe}, the highest ones those of tRNA^{Asp}. Also, in each structure the highest differences are for the atoms covalently linked to the phosphorus atoms. In restrained least squares, temperature factors are restrained by restraining the variances of the interatomic distributions to small values (Konnert & Hendrickson, 1980). Molecular-dynamics calculations have shown that the weights used to restrain neighboring-atom temperature factors in proteins (Yu, Karplus & Hendrickson, 1985; Kuriyan,

Table 1. *Summary of refinement parameters*

	OrthoPhe	MonoPhe	Asp *B*	Asp *A*
Mean F_{obs}	478·4	284·1	17·1	17·1
Mean $(F_{obs}-F_{calc})$	82·4	48·5	3·2	3·3
Final σ applied on F_{obs}	70·0	41·0	3·0	3·0
Ratio σ/F_{obs}	14·6	14·4	17·6	17·6
Mean positional shift (Å) at the end of refinement	0·012	0·011	0·016	0·037
Mean thermal shift (Å^2) at the end of refinement	0·16	0·16	0·12	0·23
R factor*	0·172	0·171	0·188	0·193
Correlation coefficient between F_{obs} and F_{calc}*	0·85	0·93	0·88	0·88
$K=\sum F_{obs}/\sum F_{calc}$	1·042	1·022	1·042	1·041
Resolution range (Å)	10·0–3·0			
Number of reflections	4508	4019	4585	4335
Number of parameters	7244	7104	6625	7257
Ratio of observations to parameters	0·6	0·6	0·7	0·6
Number of tRNA atoms†	1652	1652	1540	1689
Number of solvent atoms	127	99	116	100
Mean thermal factor (Å)	15·8	19·6	16·8	19·0

* The *R* factor is defined as

$$\sum |F_{obs}-F_{calc}|/\sum |F_{obs}|.$$

The correlation coefficient is given by the expression

$$\sum [(F_{obs}-\bar{F}_{obs})(F_{calc}-\bar{F}_{calc})]/[\sum (F_{obs}-\bar{F}_{obs})^2 \sum (F_{calc}-\bar{F}_{calc})^2]^{1/2}.$$

† There are fewer atoms in tRNA^{Asp} since the 3′ terminal -CCA end is disordered and not included.

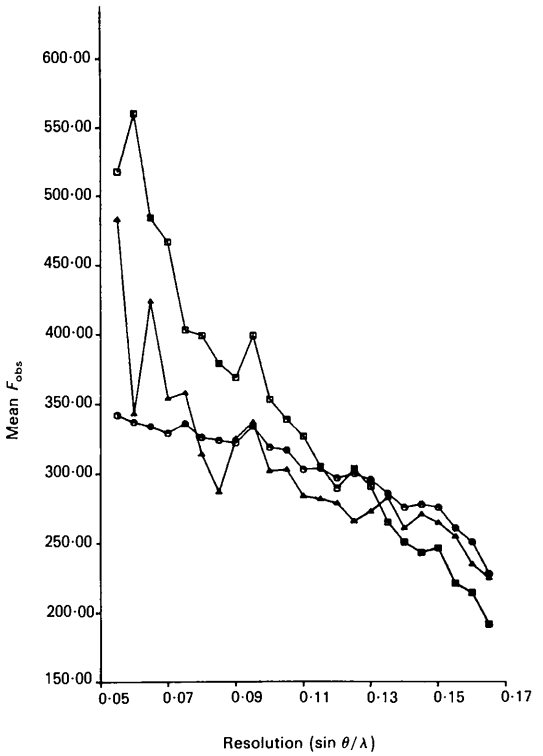

Fig. 2. Variation with resolution of the observed structure factors of each tRNA crystal: ○, orthorhombic form of yeast tRNA^{Phe}, □ monoclinic form of yeast tRNA^{Phe}, △ yeast tRNA^{Asp}. The orthorhombic form of yeast tRNA^{Phe} and yeast tRNA^{Asp} have been scaled so that the sum of the observed structure factors in each structure is equal to that of the monoclinic form of yeast tRNA^{Phe} (284). Notice the peak in the number of reflections at the resolution corresponding to the average phosphorus–phosphorus distance, 5·5 Å.

Petsko, Levy & Karplus, 1986) or in nucleic acids (Westhof, Chevrier, Weiner, Gallion & Levy, 1986) are much too restrictive. Therefore, it was decided not to use temperature-factor restraints in the last cycles. The present results show that, indeed, the differences in temperature factors of atom pairs, especially of the phosphate groups, cannot be identified with the variances of their interatomic distance distributions. However, in the early stages of refinement the use of tight restraints, on temperature factors as well as on the stereochemistry, and the monitoring of the weighted residuals are important to focus attention on particular portions of the molecular model which require further investigation.

Figs. 3 and 4 show the variation of the mean $(F_{obs}-F_{calc})$ and of the *R* factor as a function of $(\sin\theta)/\lambda$. In Fig. 3, the orthorhombic form of yeast tRNA^{Phe} shows some variation of $(F_{obs}-F_{calc})$ as a function of resolution; while, in Fig. 4, the monoclinic form of yeast tRNA^{Phe} shows the effect of the resolution on the *R* factor. For tRNA^{Asp}, the variation in both cases is weak. The curves of Figs. 3 and 4 thus reflect the curves of Fig. 2 with the data of the orthorhombic form of tRNA^{Phe} dampened at low resolution and those of the monoclinic form too weak at high resolution.

4. Occupancy and temperature factors

It was mentioned above that some residues converged to an occupancy less than unity. No attempt was made to find the other conformers, even in form *A* of yeast tRNA^{Asp} where some weak density indicated the existence of an alternative conformation for

Table 2. *Agreement statistics for geometrical parameters*

First line is for the orthorhombic form of yeast $tRNA^{Phe}$; second line for the monoclinic form; third line for the *B* form of yeast $tRNA^{Asp}$; and last line for the *A* form of yeast $tRNA^{Asp}$. The σ's applied in the refinements were the same in all structures, except in two cases for the *A* form of yeast $tRNA^{Asp}$.

Geometrical parameter	R.m.s. deviation from ideality	σ applied in the refinement
Bond distances* (Å)	0·008	
	0·008	0·02
	0·009	
	0·012	
Bond angles (°)	0·014	
	0·015	0·03
	0·014	
	0·022	
Hydrogen bonds (Å)	0·021	
	0·021	0·04
	0·019	
	0·034	
Base planarity (Å)	0·002	
	0·002	0·01
	0·002	
	0·007	0·02
Chiral volumes (Å^3)	0·017	
	0·017	0·01
	0·010	
	0·051	0·06
Single-torsion contacts (Å)	0·098	
	0·099	0·25
	0·084	
	0·107	
Multiple-torsion contacts (Å)	0·167	
	0·148	0·25
	0·166	
	0·147	
Isotropic thermal factors† (Å^2)	2·496/3·524/6·337/4·979	
	3·000/4·038/5·995/4·673	
	2·984/3·934/7·136/4·729	
	3·098/4·291/6·439/5·485	

* The number of distances deviating from ideality by more than 2σ is 23, 38, 19 and 165 respectively for the orthorhombic form of $tRNA^{Phe}$, the monoclinic form of $tRNA^{Phe}$, the *B* and the *A* forms of $tRNA^{Asp}$.

† First number is for atoms connected by a bond length, second number for atoms connected by a bond angle, third number for P–O bonds, and the fourth number for atoms involved in hydrogen bonding or in phosphate angles. No restraints were applied on the *B* factors.

residue 19. Some of the residues involved are the same in the four structures: the first and last residues (in $tRNA^{Asp}$, the last three residues are disordered), as well as residue 16 in the dihydrouridine loop (see Table 3). The other residues which have low occupancies are in the D loop for the two forms of $tRNA^{Asp}$ and in the AC loop for the two forms of $tRNA^{Phe}$. Thus, part of the D loop is disordered in $tRNA^{Asp}$ while it is a part of the AC loop which is disordered in $tRNA^{Phe}$. This is paralleled by the overall variation of temperature factors as a function of residue number, which shows high temperature factors in the AC loop of $tRNA^{Phe}$ but in the D loop of $tRNA^{Asp}$.

Fig. 5 shows the variations as a function of residue number of the phosphate-averaged temperature factors in the orthorhombic form of yeast $tRNA^{Phe}$ and in form *B* of yeast $tRNA^{Asp}$. For comparison and as a measure of the error, the difference in temperature factors of the phosphates between the two forms of $tRNA^{Phe}$ and between the two forms of $tRNA^{Asp}$ are shown in Fig. 6. The r.m.s. deviation between the temperature factors of the phosphates of the two $tRNA^{Phe}$ forms is 6·0 Å^2, while it is 3·1 Å^2 for the two $tRNA^{Asp}$ forms. Residues in three regions have higher deviations than the average in the $tRNA^{Phe}$ forms: residue 6, residues 17 and 18, and residues 66, 67 and 68. Since residue 6 is paired with residue 67, only two regions of difference exist. We have no clear explanation for these differences yet. In the $tRNA^{Asp}$ case (Fig. 6*b*) there are no significant differences in temperature factors between the two forms. From Fig. 5(*a*), it appears that the highest temperature factors in yeast $tRNA^{Phe}$ are found on the first three base pairs of the amino-acid stem, on residues 16 and 17 of the D loop, and on all residues between 25 and

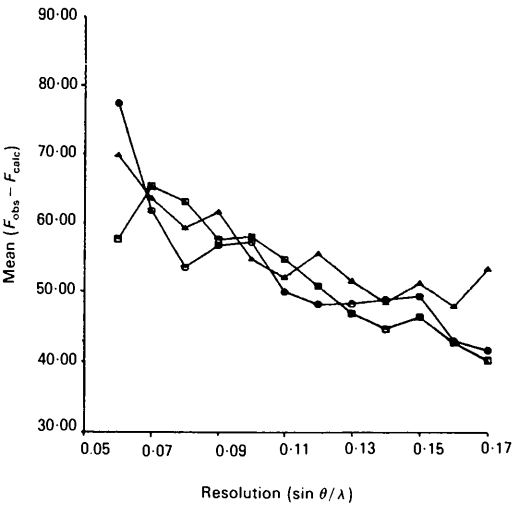

Fig. 3. Variation with resolution of the mean difference between F_{obs} and F_{calc} for the three structures (same code as for Fig. 2). The same scaling factors have been applied to the differences (F_{obs}–F_{calc}) as in Fig. 2.

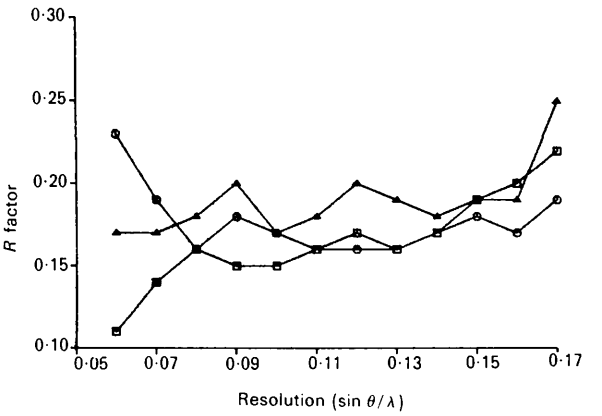

Fig. 4. Variation with resolution of the *R* factor of each structure at the end of the refinement (same code as for Fig. 2).

Table 3. *Residues with occupancies less than unity*

Residue	Group		Ortho Phe	Mono Phe		Asp *B*	Asp *A*
1	Phosphate		0·68	0·79		0·73	0·92
16	Phosphate		0·86	0·99		1·00	0·80
	Ribose		0·76	0·94		1·00	0·60
	Base	D	0·61	0·68	D	0·63	0·50
17	Phosphate		0·73	0·95			
	Ribose		0·57	0·67			
	Base	D	0·96	1·00			
18	Phosphate		1·00	1·00		1·00	0·92
	Ribose		1·00	1·00		1·00	1·00
	Base	G	1·00	1·00	G	1·00	1·00
19	Phosphate		1·00	1·00		0·91	0·78
	Ribose		1·00	1·00		0·94	0·80
	Base	G	1·00	1·00	G	0·73	0·80
20	Phosphate		1·00	1·00		0·66	0·52
	Ribose		1·00	1·00		0·65	0·30
	Base	G	1·00	1·00	D	0·65	0·20
	Phosphate					0·84	0·44
	Ribose					0·78	0·40
	Base				C	0·76	0·20
33	Phosphate		0·83	0·96		0·98	1·00
	Ribose		0·70	0·74		0·92	1·00
	Base	U	1·00	1·00	U	0·80	1·00
34	Phosphate		0·75	1·00		1·00	0·60
	Ribose		0·79	1·00		1·00	1·00
	Base	G	0·92	1·00	G	1·00	1·00
37	Phosphate		1·00	0·80		1·00	0·90
	Ribose		1·00	0·75		1·00	1·00
	Base	Y	0·67	1·00	G*	1·00	
55	Phosphate		1·00	1·00		1·00	0·90
	Ribose		1·00	1·00		1·00	0·90
	Base	P	1·00	1·00	P	1·00	0·80
76	Phosphate		0·68	0·93		0·00	0·00
	Ribose		0·62	0·93		0·00	0·00
	Base	A	0·35	0·59	A	0·00	0·00

The names of the residues in the two tRNAs are given: D, dihydrouridine; G, guanosine; Y, Y base; G*, 1-methyl-guanosine; U, uridine; P, pseudouridine; C, cytidine; A, adenosine. The CCA end of the $tRNA^{Asp}$ *B* was not included in the refinement. The nomenclature is such that the two invariant guanine bases of the D loop are 18 and 19. In $tRNA^{Asp}$, there is no residue 17, but an additional residue between 20 and 22.

49, *i.e.* the bottom half of the arm of the *L*-shaped molecule containing the AC loop. Thus, the lowest temperature factors are found in the corner of the molecule as noted by Sussman, Holbrook, Wade Warrant, Church & Kim (1978). Fig. 5(*b*) shows the temperature-factor variation as a function of residue for form *B* of $tRNA^{Asp}$. High temperature factors occur in similar regions, but with the whole D loop and only the AC-loop residues belonging to such regions. In addition, the residues of the thymine loop (T) belong also to a region with high temperature factors. This clear-cut difference between the orthorhombic form of yeast $tRNA^{Phe}$ and yeast $tRNA^{Asp}$ has already been described and discussed (Westhof, Dumas & Moras, 1983, 1985; Moras *et al.*, 1986). It is this observation which prompted the present work. The drawings of Fig. 6 show that, between the two crystalline forms of each tRNA type, the differences in temperature factors are spread equally on the whole molecule, except for the two localized regions around base pair 6-67 and base 18 in $tRNA^{Phe}$. Table 4 shows the intermolecular contacts due to the crystalline packing in $tRNA^{Phe}$ and $tRNA^{Asp}$ crystals. About the

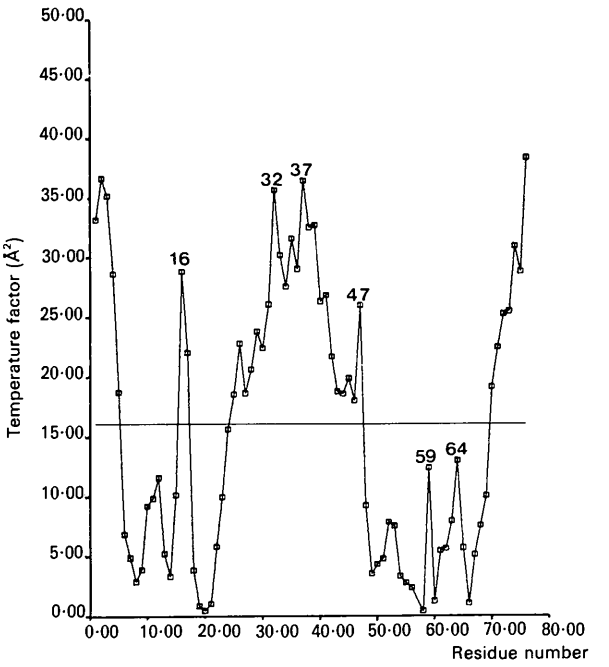

(*a*)

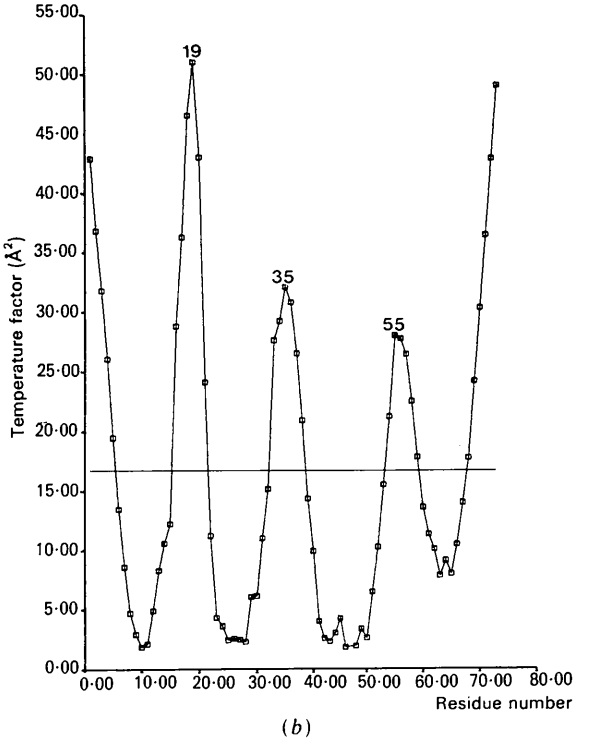

(*b*)

Fig. 5. (*a*) Variation as a function of residue number of the atomic temperature factors averaged over each residue in the orthorhombic form of yeast $tRNA^{Phe}$. (*b*) Same as in (*a*) for form *B* of yeast $tRNA^{Asp}$. The average value is indicated by a straight line.

same number of contacts are made in the four crystals. However, in the tRNA^{Phe} crystals, several contacts are made between the –CCA end (residues 74 to 76) and the minor groove of the anticodon stem. This is not the case in tRNA^{Asp} crystals where the –CCA end is disordered. The main difference between the monoclinic and the orthorhombic forms of tRNA^{Phe} is that, in the latter, base 34 interacts through symmetry-related stacking interactions with itself while, in the former, base 34 is in van der Waals contact with the sugar-phosphate backbone of A62–C63 in the T stem. In the tRNA^{Asp} crystals, the anticodon triplets of symmetry-related molecules form hydrogen-bonded base pairs. The anticodon–anticodon interactions lead to a continuous helix from one AC stem to the symmetry-related one *via* stacking at the 3′ end of each strand of the three-base-pair mini helix. Such an interaction is expected to stabilize the AC loop and stem and decrease their temperature factors. However, the change in mobility at the D- and T-loop levels is unexpected. From Table 4, it is difficult to attribute this effect exclusively to packing considerations. Thus, it would appear that the change in flexibility from the AC loop in tRNA^{Phe} to the D and T loops in tRNA^{Asp} is a consequence of the anticodon–anticodon interactions.

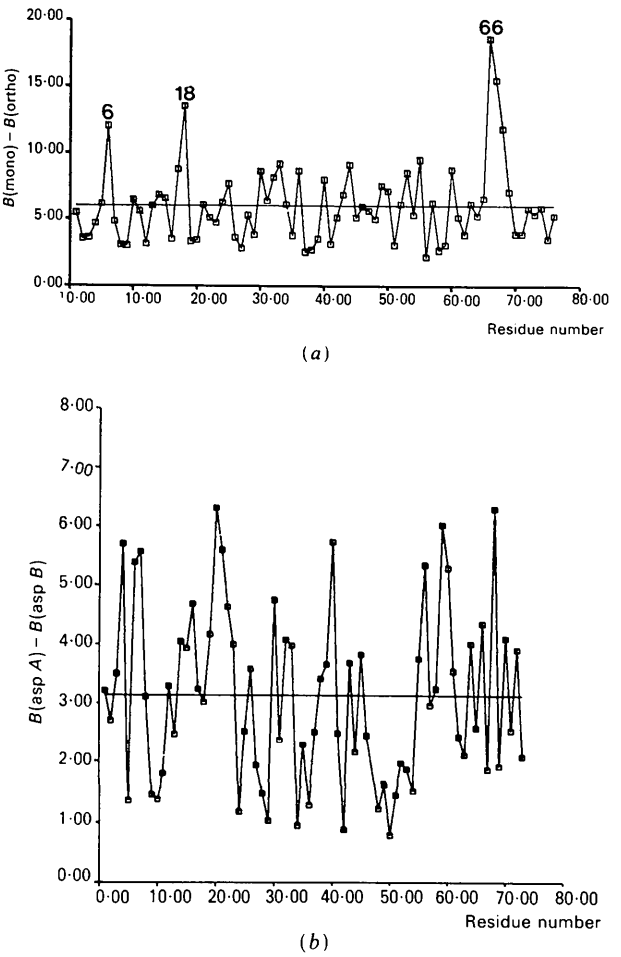

Fig. 6. (*a*) Variation as a function of residue number of the difference between the residue-averaged temperature factors of yeast tRNA^{Phe} in the monoclinic and orthorhombic forms. (*b*) The same for forms *A* and *B* of yeast tRNA^{Asp}. Notice the different scales. The average difference is indicated by a straight line.

Table 4. *Packing contacts* (<3·5 Å) *in the tRNA crystals*

Residue 1	Residue 2	Code*	Number of contacts	Interactions†
Orthorhombic form of yeast tRNA^{Phe}				
5	53	1, −1 0 0	2	H bond
34	34	2, 0 0 0	13	Base stacking
20	56	3, −1 0 0	25	Base stacking
28	75	3, 0 1 0	8	
42-44	75-76	3, 0 1 0	12	H bonds
37	76	3, −1 1 0	4	H bond
Total number of contacts			64	
(without –CCA end)			40	
Monoclinic form of yeast tRNA^{Phe}				
5	53	1, 0 −1 0	1	H bond
34	62	1, 0 −1 −1	4	Base on sugar
30	75-76	2, 1 0 1	13	
42-43	75-76	2, 1 0 1	31	H bonds
20	56	2, 2 −1 1	19	Base stacking
Total number of contacts			68	
(without –CCA end)			24	
Form *A* of yeast tRNA^{Asp}				
10/26	49/50	2, 0 0 0	8	H bonds
34-37	34-37	4, 0 0 −1	11	Base pairing
1	56/18	5, 0 −1 0	17	Sugar on base
19	72-73	5, −1 0 0	3	
5	41	6, 0 0 0	6	Sugar-sugar
16	28-29	6, 0 0 0	6	H bonds
31	62	6, −1 0 0	1	
Total number of contacts			52	
Form *B* of yeast tRNA^{Asp}				
10	49	2, 0 0 0	11	H bonds
34-37	34-37	4, 0 0 −1	24	Base pairing
1	56	5, 0 −1 0	22	Sugar on base
20	68	5, −1 0 0	8	
4	41	6, 0 0 0	8	Sugar-sugar
31	61	6, −1 0 0	2	
Total number of contacts			75	

* The symmetry operation to be applied on the second residue. The first number refers to one of the transformations below and the three subsequent numbers to the translation along *x*, *y*, *z*. tRNA^{Phe}: For the orthorhombic form: (1) *x*, *y*, *z*; (2) $-x$, *y*, $-z$; (3) $0{\cdot}5+x$, $-y$, $0{\cdot}5-z$. For the monoclinic form: (1) *x*, *y*, *x*; (2) $-x$, $0{\cdot}5+y$, $-z$. For tRNA^{Asp}: (2) *x*, $-y$, $-z$; (4) $-x$, *y*, $0{\cdot}5-z$; (5) $0{\cdot}5+x$, $0{\cdot}5+y$, *z*; (6) $x+0{\cdot}5$, $0{\cdot}5-y$, $-z$.

† Types of interactions besides van der Waals contacts. The conformation of the anticodon triplet is different in the two forms of yeast tRNA^{Asp}: in form *A*, there are hydrogen bonds between the two central uridines with twofold disorder while, in form B, the uridines are symmetrically disposed with no interactions. These two situations cannot be distinguished crystallographically.

5. Internal mobility

Of the three main groups which constitute a nucleotide, phosphate, sugar and base, the phosphate group tends to have the highest thermal factor (Sussman *et al.*, 1978). However, the exceptions to this rule are

interesting. Fig. 7 shows the difference between the group temperature factors of the phosphate and the base in the orthorhombic form of $tRNA^{Phe}$ and in form *B* of $tRNA^{Asp}$. From Fig. 7, it appears first that the extremes in variation are about twice as large in $tRNA^{Phe}$ than in $tRNA^{Asp}$ and, secondly, that the regions where the bases are more mobile are not the same, except for residue 16. It is difficult to rationalize the first observation. It could be due to the different dependence on resolution of the diffraction data (see Fig. 2). Alternatively, it is possible that such a difference in internal mobility might arise from the very different crystallization conditions: $tRNA^{Phe}$ was crystallized at a lower ionic strength than $tRNA^{Asp}$ (Dock *et al.*, 1984). Notice also that the average of the difference is displaced towards the positive values in $tRNA^{Phe}$, while it is close to zero in $tRNA^{Asp}$. Thus, on the average, the statement that phosphates are more mobile than the bases is more appropriate to $tRNA^{Phe}$ than to $tRNA^{Asp}$. The fact that bases 16 and 47 are more mobile than their phosphates is understandable since these bases protrude from the surface of the molecule. However, in $tRNA^{Phe}$ all the bases of the D stem and of the D loop are more mobile than their phosphates. This is not the case in $tRNA^{Asp}$ where only the bases 16, 17 and 18 are more mobile than their phosphates and where the phosphates of the D stem are either more mobile than their bases or have the same mobility. It is not clear whether this observation is related to the differences in times of hydrogen exchange of imino protons in base pairs in the D stem as measured by NMR (Roy & Redfield, 1983; Figuerova, Keith, Leroy, Plateau, Roy & Gueron, 1983).

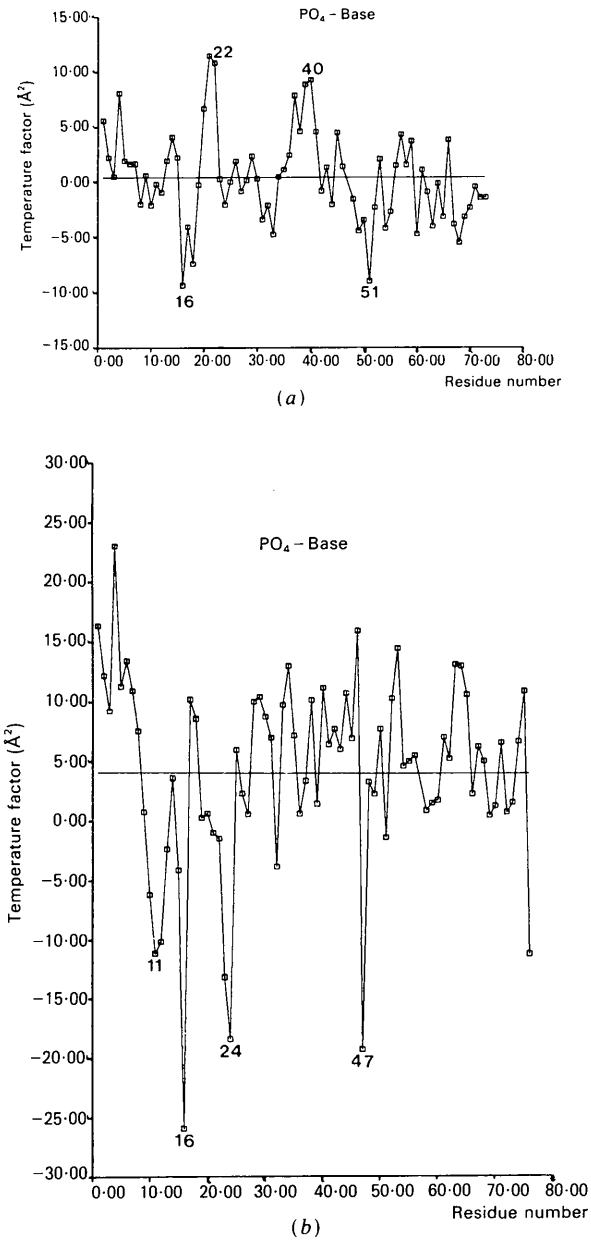

Fig. 7. (*a*) Variation as a function of residue number of the difference between the group-averaged temperature factors of the phosphate and base in the orthorhombic form of yeast $tRNA^{Phe}$. (*b*) Same as in (*a*) for form *B* of $tRNA^{Asp}$. The average difference is indicated by a straight line.

6. Relative atomic displacement between the structures

Fig. 8 shows the displacement between the phosphorus-atom positions of the previously refined structure of the orthorhombic form of yeast $tRNA^{Phe}$ (Sussman *et al.*, 1978) and after the present refinement as well as the displacement between the phosphorus-atom positions of the present refinement of the two forms of yeast $tRNA^{Phe}$. The overall r.m.s. difference between the previous and present refinements of the orthorhombic form of $tRNA^{Phe}$ is 0·43 Å, while it is 0·77 Å between the two forms of $tRNA^{Phe}$, *i.e.* about twice as much. A similar overall r.m.s. difference was found between the two refinements of the monoclinic form of $tRNA^{Phe}$, 0·48 Å (Westhof & Sundaralingam, 1986). The phosphates with the largest differences are those of residues 38 and 46 (1·2 and 1·0 Å, respectively) closely followed by residues 34 and 16–17 (0·9, 0·8 and 0·7 Å, respectively). These residues have high temperature factors and low occupancies. It is therefore not surprising that their determination is less precise. Between the two forms of $tRNA^{Phe}$, the largest deviations are localized to the first four residues at the 5′ end, to the last four at the 3′ end, and to residues 34 and 35. Again, these residues are in regions with high temperature factors in both forms and either are not well determined in both forms or have slightly different average conformations owing to the different crystal environments. Again, as for the temperature factors, no effect of crystalline packing on the molecular structure of yeast $tRNA^{Phe}$ can be detected. Fig. 9 shows a similar distance plot for

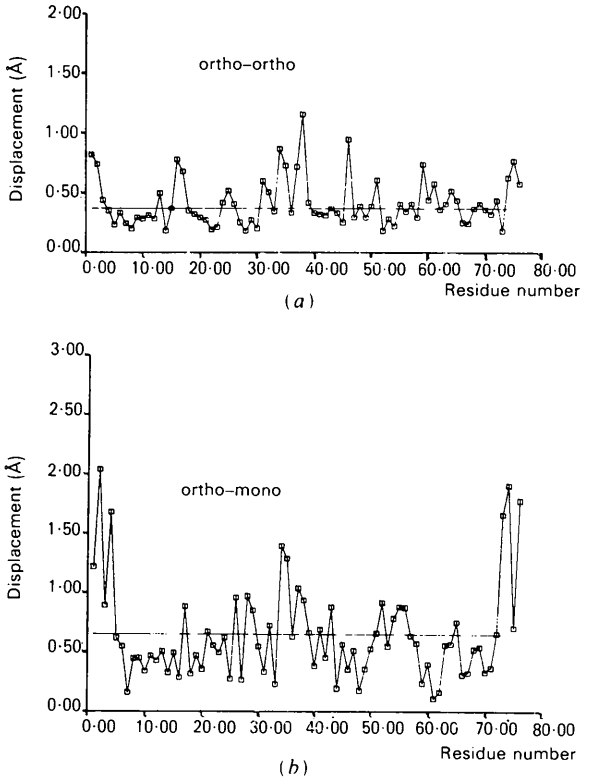

Fig. 8. (*a*) Variation as a function of residue number of the distance between homologous phosphorus atoms of the previous (Sussman *et al.*, 1978) and present refinements of the orthorhombic form of yeast $tRNA^{Phe}$. (*b*) Variation as a function of residue number of the distance between homologous phosphorus atoms in the orthorhombic and monoclinic forms of yeast $tRNA^{Phe}$.

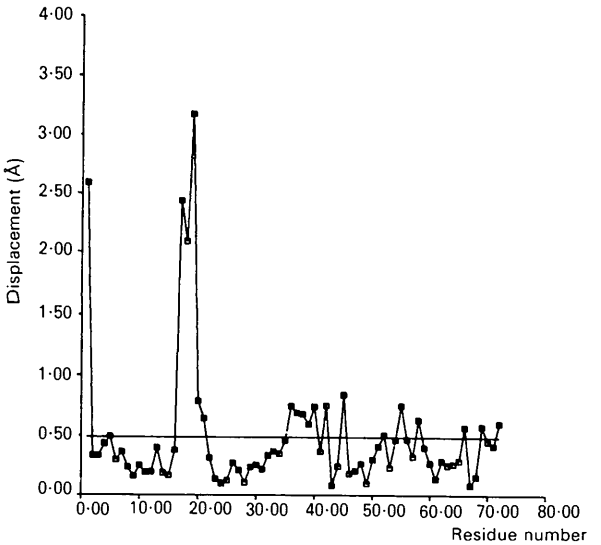

Fig. 9. Variation as a function of residue number of the distance between homologous phosphorus atoms in form *A* and form *B* of $tRNA^{Asp}$.

the two forms of yeast $tRNA^{Asp}$. A large conformational change in the D loop is apparent, besides that of the phosphorus atom of residue 1. While there are no tertiary interactions between one invariant guanine of the D loop (G19) and the invariant cytosine of the T loop (C56) in form *B*, such an interaction is present in form *A* (Dumas, Westhof & Moras, 1988). This change in the D loop leads to an overall r.m.s. difference between the two forms of 0·69 Å. Most of the other phosphorus atoms have displacements less than 0·50 Å, except for residues 36 and up of one strand of the AC stem.

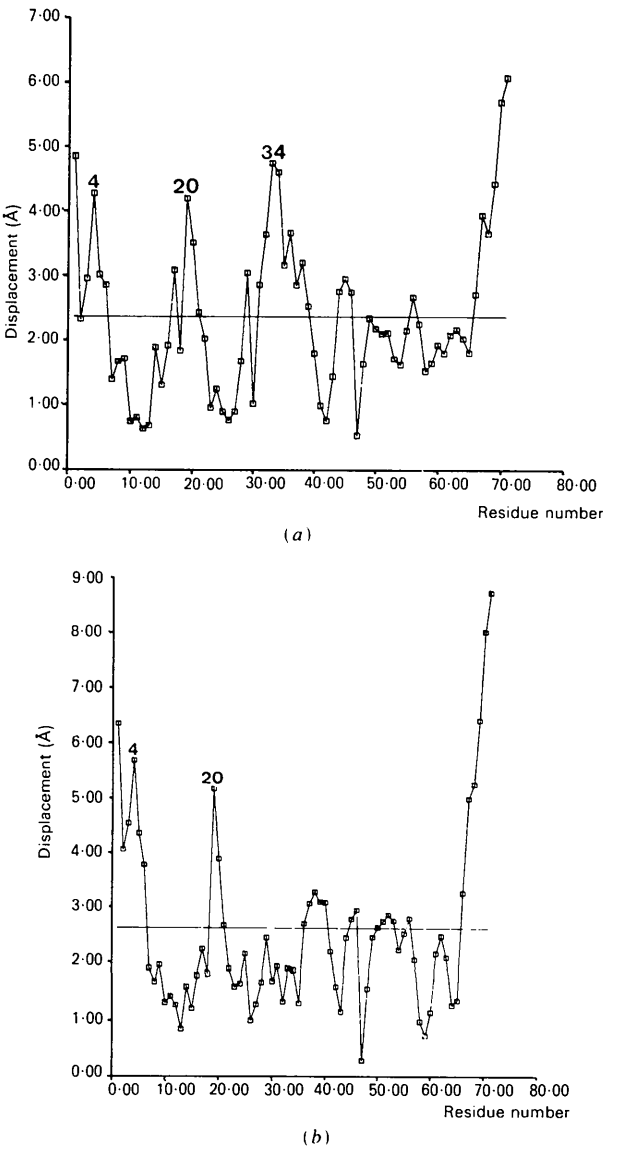

Fig. 10. (*a*) Distance between homologous phosphorus atoms after least-squares superposition of yeast $tRNA^{Asp}$ and the orthorhombic form of yeast $tRNA^{Phe}$ as a function of residue number. (*b*) Same as in (*a*), but the fit between the two structures is obtained after superposition of the inertial axis system. The average difference is indicated by a straight line.

Fig. 10 shows the relative distance between the phosphorus atoms of the orthorhombic form of $tRNA^{Phe}$ and form *B* of $tRNA^{Asp}$ after two methods of superposition. For the superpositions, residue D17 has been removed from the $tRNA^{Phe}$ coordinates and residue 20 from the $tRNA^{Asp}$ coordinates so that the two invariant guanines of the D loop are superposable. Also, since the CCA end was not observed in the crystal of yeast $tRNA^{Asp}$, the CCA end was removed from the structure of yeast $tRNA^{Phe}$, as well as residue 47, which is not present in yeast $tRNA^{Asp}$. The two structures were first superposed by least squares without allowing for deformation or giving more weight to some parts of the molecules. The overall r.m.s. difference between the two structures is 2·6 Å. Again, the deviations occur at the beginning of the amino-acid stem (first and last six residues), in the D loop (residues 18 to 21), and in the AC stem and loop (residues 30–40, thus below the G-U pair). In addition, there are some lesser deviations at the level of the variable loop (residues 45–48). Interestingly, the lowest deviations are observed for the D stem, at the beginning of the AC loop, and for phosphate 49, *i.e.* in the core of the molecule.

The two structures have been superposed by another method. In this second method, each structure is set in its inertial system and then, in that axis system, the distances between the phosphates are calculated. The result is given in Fig. 10(*b*). The main differences between the two curves of Fig. 10 reside in the region of the AC stem and loop and at the end of the other arm of the *L*-shaped molecule. In the anticodon region, the distance between corresponding phosphates has been reduced and at the end of the amino-acid stem there is a larger distance between the phosphates. Interestingly, the same minima in the displacement are found in the two curves: at phosphates 13, 27 and 49. The stereo drawing of Fig. 11 shows the superposition in the inertial system where the fit is best along the largest moment of inertia which is along the anticodon arm with the largest differences in the AA stem. From Fig. 11 it appears that the widening of the angle formed by the two branches of the *L* in $tRNA^{Asp}$ (Moras *et al.*, 1980) is due to a kink at the junction between the T and AA stems (Dumas *et al.*, 1985).

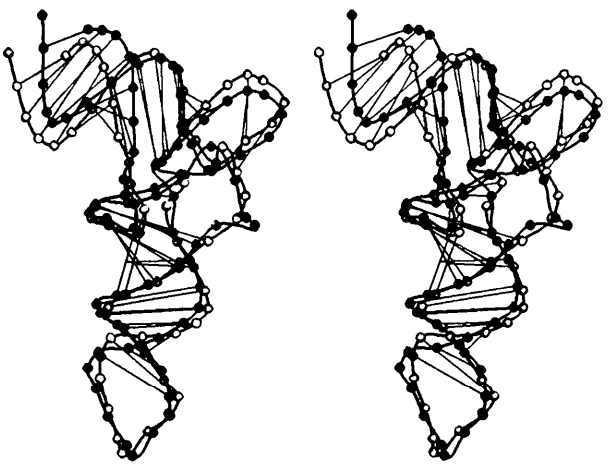

Fig. 11. Stereo views of the two structures after superposition in their inertial system (black circles: yeast $tRNA^{Asp}$; unfilled circles: yeast $tRNA^{Phe}$).

7. Local geometry: twist, propeller twist and roll

The global twist between two base pairs is the angle between the vectors connecting the C1′ atoms of each base in a base pair viewed in projection down the helical axis (Fratini, Kopka, Drew & Dickerson, 1982). The propeller twist of a base pair is the angle between the mean planes of the bases (viewed along the long axis, a clockwise rotation of the nearer base is considered a positive propeller twist). Roll is the relative angle of rotation between two base pairs along their long axis (positive when opening up in the major groove). Tilt, the relative angle of rotation between base pairs along their short axis, is close to zero in all structures and is not discussed here. Fig. 12 shows the twist and propeller-twist variations in the helical stems of the orthorhombic form of yeast $tRNA^{Phe}$ with the previous (Sussman *et al.*, 1978) and the present refinements. It can be seen that the absolute values and the variation of the twist are essentially identical after the two refinements. For the propeller twist, the absolute values in the amino-acid stem after the present refinement are larger than those obtained after the previous refinement, but the variations are very much the same. Larger differences are, however, observed for the thymine and dihydrouridine stems.

Fig. 13 shows the twist and propeller twist for the monoclinic form of yeast $tRNA^{Phe}$ and form *B* of

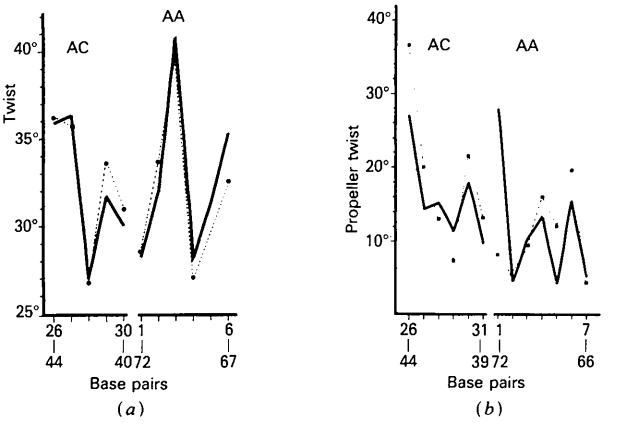

Fig. 12. Variation of the twist (*a*) and propeller twist (*b*) of the base pairs of the anticodon and amino-acid stems in the orthorhombic form of yeast $tRNA^{Phe}$ for the present refinement (thick lines) and the previous refinement of Sussman *et al.* (1978) (black dots). The twist of each base pair on the following one is represented.

yeast $tRNA^{Asp}$ after the present refinement. Two observations can be made on this figure. First, the variations in twist are clearly different in $tRNA^{Phe}$ and $tRNA^{Asp}$ in the the AC and AA stems. Notice especially the effect of the G-U pair in the amino-acid stem. In $tRNA^{Phe}$ the largest twist occurs between the preceding base pair and the G4-U69 pair, while in $tRNA^{Asp}$ the largest twist occurs between the U5-G68 pair and the following base pair. The importance of the position of the G in G-U pair has already been discussed (Mizuno & Sundaralingam, 1978; Westhof, Dumas & Moras, 1985). However, in the AC stem the different variations in twist cannot be explained by the presence of the G-U pair, G30-U40, present in $tRNA^{Asp}$ and absent in $tRNA^{Phe}$, since the variations in twist around that region are quite similar. In fact, from the example of the AA stem, one would expect quite a difference at that position. The differences in twist variations in the AC stem seem, therefore, to need another explanation (see below). Secondly, the variations of propeller twist in the three structures are similar, especially in the anticodon stem with a minimum at 29-41 and a maximum at 30-40. It is interesting that 29-41 is always a Watson-Crick base pair (Grosjean, Cedergreen & McKay, 1982). The variation in the amino-acid stem in $tRNA^{Asp}$ and the monoclinic form of $tRNA^{Phe}$ is also very similar. The orthorhombic form of $tRNA^{Phe}$ is different from the other two structures most probably because of the different conformations at the level of the sugar-phosphate backbone of G4 (this is apparent also in Figs. 8 and 11). Interestingly, the roll angle in the AC and AA stems is also quite similar in the two types of tRNAs. Large roll angles are observed at the beginning of the AC stem (between base pairs 26-44 and 27-43) and at the end of the AA stem (between base pairs 6-67 and 7-66). Both regions are at the interface between two stems, the D and AC stems and the T and AA stems, respectively. Also, a maximum in the roll angle is observed at the third base pair of the AA stem in $tRNA^{Phe}$ and $tRNA^{Asp}$.

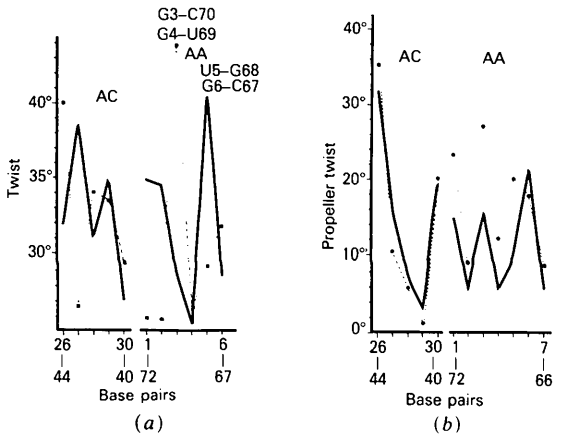

Fig. 13. Variation of the twist (*a*) and propeller twist (*b*) of the base pairs of the anticodon and amino-acid stems in the monoclinic (black squares connected by dotted lines) form of yeast $tRNA^{Phe}$ as well as in yeast $tRNA^{Asp}$ (thick lines). The positions of the G-U pairs in the AA stem of yeast $tRNA^{Phe}$ and $tRNA^{Asp}$ are indicated.

8. Concluding remarks

Crystallographically, the refinement of these four structures proceeded in a very similar way, apart from specific modelling errors. This is in striking contrast to what was observed with some smaller DNA oligomers where each structure behaved differently during the refinement (Westhof, Prange, Chevrier & Moras, 1985). The lower resolution of the present study, together with the similarity in diffraction data, might explain the similarity in refinement behavior of the tRNA structures. The structure of the orthorhombic form of yeast $tRNA^{Phe}$ obtained after the present refinement is very close to that obtained after the *CORELS* refinement. It is apparent, however, that the local geometry as determined by absolute values of twist and propeller twist is very dependent on the refinement program employed and on real-space modelling, although the variations are not.

The four structures described here present, beyond the overall resemblance due to the *L*-shaped tertiary folding, striking similarities and stark differences at one and the same time. While the D and AC loops have a tendency towards large temperature factors and low occupancies in all tRNAs, they present inverse relative distributions in $tRNA^{Asp}$ and $tRNA^{Phe}$, with a decrease in overall mobility of the AC loop and an increase of the D- and T-loop mobility in $tRNA^{Asp}$ compared with $tRNA^{Phe}$. Those crystallographic results explain the self-splitting patterns of $tRNA^{Asp}$ in crystals, where the D loop is chemically fragile, and in solution, where major cuts are observed in the AC loop (Moras *et al.*, 1986). Indeed, in solution in the absence of ammonium sulfate, the $tRNA^{Asp}$ molecules do not exist as dimers (Romby, Giegé, Houssier & Grosjean, 1985). Also, on the one hand, the base-pair roll and propeller twist of some stems have similar variations in all tRNAs, while on the other hand, the variations in base-pair twist are strongly different between $tRNA^{Asp}$ and $tRNA^{Phe}$.

In previous work (Westhof, Dumas & Moras, 1985; Moras *et al.*, 1986; Giegé, Huong & Moras, 1986; Dumas, Westhof & Moras, 1988), it was suggested that the different distribution of temperature factors in the two structures, *i.e.* the transfer of flexibility from the anticodon loop to the thymine and dihydrouridine loops seen in $tRNA^{Asp}$, results from the base pairing between symmetrically related anticodon triplets in the structure of $tRNA^{Asp}$. The present analysis could indicate that the occurrence of base pairing in the anticodon loop, *via* base stacking of residues 37 and 38, leads to a propagation of twist

variation through the anticodon stem, provoking a labilization of the interactions between the T and D loops. However, mechanical processes involving coupling between other degrees of freedom in the tRNA dimer might be implicated.*

We are grateful to Professors S. H. Kim (Berkeley University) and M. Sundaralingam (University of Wisconsin) for giving us their X-ray data on, respectively, the orthorhombic and monoclinic form of yeast $tRNA^{Phe}$. This work would not have been possible without their collaboration. We thank R. E. Dickerson (UCLA), W. A. Hendrickson (Columbia University), W. K. Olson (Rutgers University), G. J. Quigley (MIT) and S. T. Rao (University of Wisconsin) for the use of their programs and for discussions. The authors acknowledge fruitful discussions with their colleagues, especially R. Giegé, P. Romby, J. C. Thierry and are grateful to Professor J. P. Ebel for his constant interest, encouragement, and support.

* Atomic coordinates and structure factors of the *A* form of $tRNA^{Asp}$ (Reference: 2TRA, R2TRASF) and the *B* form of $tRNA^{Asp}$ (3TRA, R3TRASF), and the present atomic coordinates of the orthorhombic form of $tRNA^{Phe}$ (4TRA) have been deposited with the Protein Data Bank, Brookhaven National Laboratory and are available in machine readable form from the Protein Data Bank at Brookhaven or one of the affiliated centres at Melbourne or Osaka. The data have also been deposited with the British Library Document Supply Centre as Supplementary Publication No. SUP 37021 (as microfiche). Free copies may be obtained through The Executive Secretary, International Union of Crystallography, 5 Abbey Square, Chester CH1 2HU, England.

References

ALTONA, C. & SUNDARALINGAM, M. (1972). *J. Am. Chem. Soc.* **94**, 8205-8209.

DOCK, A. C., LORBER, B., MORAS, D., PIXA, G., THIERRY, J. C. & GIEGÉ, R. (1984). *Biochimie*, **66**, 179-201.

DUMAS, P., EBEL, J. P., GIEGÉ, R., MORAS, D., THIERRY, J. C. & WESTHOF, E. (1985). *Biochimie*, **67**, 597-606.

DUMAS, P., WESTHOF, E. & MORAS, D. (1988). Submitted to *J. Biol. Chem.*

FIGUEROVA, N., KEITH, G., LEROY, J. L., PLATEAU, P., ROY, F. & GUERON, M. (1983). *Proc. Natl Acad. Sci. USA*, **80**, 4330-4333.

FRATINI, A. V., KOPKA, M. L., DREW, H. & DICKERSON, R. E. (1982). *J. Biol. Chem.* **257**, 14686-14707.

GIEGÉ, R., HUONG, P. V. & MORAS, D. (1986). *Spectrochim. Acta Part A*, **42**, 387-392.

GROSJEAN, H., CEDERGREEN, R. J. & MCKAY, W. (1982). *Biochimie*, **64**, 387-397.

HENDRICKSON, W. A. & KONNERT, J. H. (1980). *Biomolecular Structure, Function, Conformation and Evolution*, edited by R. SRINIVASAN, Vol. 1, pp. 43-57. Oxford: Pergamon Press.

HINGERTY, B., BROWN, R. S. & JACK, A. (1978). *J. Mol. Biol.* **124**, 523-534.

JACK, A. & LEVITT, M. (1978). *Acta Cryst.* A**34**, 931-935.

KONNERT, J. H. (1976). *Acta Cryst.* A**32**, 614-617.

KONNERT, J. H. & HENDRICKSON, W. A. (1980). *Acta Cryst.* A**36**, 344-350.

KURIYAN, J., PETSKO, G. A., LEVY, R. M. & KARPLUS, M. (1986). *J. Mol. Biol.* **190**, 227-254.

MERRITT, E. A. & SUNDARALINGAM, M. (1985). *J. Biomol. Struct. Dyn.* **3**, 559-578.

MIZUNO, H. & SUNDARALINGAM, M. (1978). *Nucl. Acids Res.* **5**, 4451-4461.

MORAS, D., COMARMOND, M. B., FISCHER, J., WEISS, R., THIERRY, J. C., EBEL, J. P. & GIEGÉ, R. (1980). *Nature (London)*, **288**, 669-674.

MORAS, D., DOCK, A. C., DUMAS, P., WESTHOF, E., ROMBY, P., EBEL, J. P. & GIEGÉ, R. (1986). *Proc. Natl Acad. Sci. USA*, **83**, 932-936.

QUIGLEY, G. J., TEETER, M. M. & RICH, A. (1978). *Proc. Natl Acad. Sci. USA*, **75**, 64-68.

ROMBY, P., GIEGÉ, R., HOUSSIER, C. & GROSJEAN, H. (1985). *J. Mol. Biol.* **184**, 107-118.

ROY, S. & REDFIELD, A. G. (1983). *Biochemistry*, **22**, 1386-1390.

STOUT, C. D., MIZUNO, H., RAO, S. T., SWAMINATHAN, P., RUBIN, J., BRENNAN, T. & SUNDARALINGAM, M. (1978). *Acta Cryst.* B**34**, 1529-1544.

SUNDARALINGAM, M. (1969). *Biopolymers*, **7**, 821-860.

SUSSMAN, J. L., HOLBROOK, S. R., CHURCH, G. M. & KIM, S. H. (1977). *Acta Cryst.* A**33**, 800-804.

SUSSMAN, J. L., HOLBROOK, S. R., WADE WARRANT, R., CHURCH, G. M. & KIM, S. H. (1978). *J. Mol. Biol.* **123**, 607-630.

WASER, J. (1963). *Acta Cryst.* **16**, 1091-1094.

WESTHOF, E., CHEVRIER, B., WEINER, P. K., GALLION, S. L. & LEVY, R. L. (1986). *J. Mol. Biol.* **191**, 699-712.

WESTHOF, E., DUMAS, P. & MORAS, D. (1983). *J. Biomol. Struct. Dyn.* **1**, 337-355.

WESTHOF, E., DUMAS, P. & MORAS, D. (1985). *J. Mol. Biol.* **184**, 119-145.

WESTHOF, E. DUMAS, P. & MORAS, D. (1988). Submitted to *Biochimie.*

WESTHOF, E., PRANGE, TH., CHEVRIER, B. & MORAS, D. (1985). *Biochimie*, **67**, 811-817.

WESTHOF, E. & SUNDARALINGAM, M. (1983). *Structure and Dynamics: Nucleic Acids and Proteins*, edited by E. CLEMENTI & R. H. SRAM, pp. 135-147. New York: Adenine Press.

WESTHOF, E. & SUNDARALINGAM, M. (1986). *Biochemistry*, **25**, 4868-4878.

YU, H., KARPLUS, M. & HENDRICKSON, W. A. (1985). *Acta Cryst.* B**41**, 191-201.

Acta Cryst. (1988). A44, 124–127

Etude des Représentations des Groupes Ponctuels Bicolores Cristallographiques Sous-Tendues par des Familles de Points Equivalents*

PAR JAMIL BELGUITH ET YVES BILLIET†

Ecole Nationale d'Ingénieurs de Sfax, BP W, 3038 Sfax, Tunisie

(*Reçu le* 17 *décembre* 1985, *accepté le* 4 *septembre* 1987)

Abstract

The representations spanned by sets of equivalent (general or special) positions of the crystallographic coloured point groups are reduced to irreducible representations using a property proposed by Bates [Labarre (1978). *Théorie des Groupes.* Paris: Presses Universitaires de France]. The derivation has been carried out fully for the 32 one-coloured point groups, for the 58 true two-coloured point groups and the 32 grey point groups. Examples of groups $\bar{4}\,2\,m$, $2/m\,2/m\,2/m$; $2'/m\,2'/m\,2/m'$; $2'/m'\,2'/m'\,2/m$; $2/m'\,2/m'\,2/m'$ and $2/m\,2/m\,2/m\,1'$ are given.

I. Introduction

La représentation sous-tendue par les vecteurs joignant le point central‡ d'un groupe ponctuel aux positions d'une famille générale de points équivalents est bien connue: c'est la représentation régulière. Cette représentation a pour dimension l'ordre du groupe et dans sa réduction figure chaque représentation irréductible affectée d'un poids égal à sa dimension. Ainsi la représentation sous-tendue par une famille générale de positions du groupe ponctuel monocolore $\bar{4}\,2\,m$ est de dimension 8 et sa réduction selon les représentations irréductibles de $\bar{4}\,2\,m$ est $A_1+A_2+B_1+B_2+2E$. Les représentations A_1, A_2, B_1, B_2 sont de dimension 1 et la représentation E est de dimension 2. A l'exception de quelques tentatives antérieures, notamment celles de Bertaut (1968, 1981), il ne semble pas que les représentations sous-tendues par les vecteurs joignant le point central aux positions des familles spéciales aient fait l'objet d'étude complète ni pour les groupes ponctuels ordinaires (monocolores) ni pour les groupes ponctuels colorés (bicolores et gris).* Cette étude est systématiquement faite ici. Rappelons que les groupes ponctuels magnétiques sont isomorphes des groupes colorés à 2 couleurs au plus; il existe donc une correspondance biunivoque entre les représentations de ces groupes (*cf.* Bertaut, 1968).

II. Méthode employée

La méthode classique de réduction d'une représentation a été étendue sans difficulté aux représentations sous-tendues par les familles spéciales. Rappelons le principe sur l'exemple du groupe monocolore $\bar{4}\,2\,m$.

Considérons la famille spéciale $4\,n$ comprenant quatre positions

$$4\,n\,..\,m \quad (1)\ x, x, z, t;\ (2)\ x, \bar{x}, \bar{z}, t;$$
$$(3)\ \bar{x}, x, \bar{z}, t;\ (4)\ \bar{x}, \bar{x}, z, t.$$

On est amené dans le cas des groupes colorés, à 2 couleurs au plus, à donner quatre coordonnées x, y, z, t aux positions des familles générales et spéciales; les trois premières sont les coordonnées géométriques habituelles, la quatrième donne la couleur. Dans le cas d'un groupe monocolore la quatrième coordonnée ne prend qu'une valeur dans chaque famille, tandis que dans le cas d'un groupe bicolore vrai ou gris, cette coordonnée peut prendre deux valeurs opposées dans chaque famille de Wyckoff. L'opération $\bar{4}^3$ transforme les vecteurs définissant les positions comme suit:

$$(1)\ x, x, z, t \rightarrow (3)\ \bar{x}, x, \bar{z}, t$$
$$(2)\ x, \bar{x}, \bar{z}, t \rightarrow (1)\ x, x, z, t$$
$$(3)\ \bar{x}, x, \bar{z}, t \rightarrow (4)\ \bar{x}, \bar{x}, z, t$$
$$(4)\ \bar{x}, \bar{x}, z, t \rightarrow (2)\ x, \bar{x}, \bar{z}, t.$$

* An English translation 'not refereed' may be obtained from the authors upon request.

† A qui doit être adressée toute correspondance.

‡ Par définition, un groupe ponctuel laisse invariant au moins un point de l'espace; pour certains groupes (par exemple $6/m'$) ce point est unique; pour d'autres les points invariants sont en nombre infini situés sur une droite (par exemple $6m'm'$) ou sur un plan (par exemple m'). On appelle point central, le point invariant origine du repère conventionnel.

* On trouvera dans Bertaut (1968) un procédé très simple de construction des groupes bicolores à partir de la table des caractères du groupe monocolore dont ils dérivent: il existe une correspondance biunivoque entre les représentations irréductibles unidimensionnelles alternées du groupe monocolore et celles des groupes bicolores associés.

0108-7673/88/020124-04$03.00